DNA translocating through a carbon nanotube can increase ionic current

2012 Nanotechnology 23 455107

(http://iopscience.iop.org/0957-4484/23/45/455107)

Nanotechnology **23** (2012) 455107 (6pp) doi:10.1088/0957-4484/23/45/455107

DNA translocating through a carbon nanotube can increase ionic current

Jae Hyun Park[1,2], Jin He[3,4], Brett Gyarfas[4], Stuart Lindsay[4,5,6] and Predrag S Krstić[1,7,8,9]

[1] Physics Division, Oak Ridge National Laboratory, Oak Ridge, TN 37831, USA
[2] Department of Aerospace and System Engineering, Gyeongsang National University, Jinju, Gyeongnam 660-701, Korea
[3] Physics Department, Florida International University, Miami, FL 33199, USA
[4] Biodesign Institute, Arizona State University, Tempe, AZ 85287, USA
[5] Department of Physics, Arizona State University, Tempe, AZ 85287, USA
[6] Department of Chemistry and Biochemistry, Arizona State University, Tempe, AZ 85287, USA
[7] Joint Institute of Computational Science, University of Tennessee, Oak Ridge, TN 37831, USA
[8] Department of Physics and Astronomy, University of Tennessee, Knoxville, TN 37006, USA

E-mail: pkrstic@utk.edu

Received 3 July 2012, in final form 19 September 2012
Published 22 October 2012
Online at stacks.iop.org/Nano/23/455107

Abstract
Translocation of DNA through a narrow, single-walled carbon nanotube can be accompanied by large increases in ion current, recently observed in contrast to the ion current blockade. We use molecular dynamics simulations to show that large electro-osmotic flow can be turned into a large net current via ion-selective filtering by a DNA molecule inside the carbon nanotube.

S Online supplementary data available from stacks.iop.org/Nano/23/455107/mmedia

(Some figures may appear in colour only in the online journal)

1. Introduction

The next step in advancement of DNA sequencing technology is third generation sequencing, based on single-molecule, voltage-driven transport through biological and synthetic nanopores [1]. These nanopores provide localization and controlled motion for sequence recognition of single DNA molecules. Typically, a DNA polymer, negatively charged in a solution, translocates through a nanopore under an externally applied electric field, caused by the electrophoretic voltage bias. The nanopore is sandwiched between two reservoirs, which supply ionic solution as well as the DNA segments for translocation.

DNA translocation through a nanopore is usually detected via a fall in ionic current, since DNA may mechanically block a number of charge carriers in the nanopore. Fan *et al* [2] showed how small increases in nanopore current can occur at lower salt concentrations and be accounted for by the counterions pulled into a channel by translocating DNA. On the other hand, positively charged counterions can form an electrical double layer (EDL) around DNA, which when exposed to the electrophoretic driving force may contribute to an increase of electro-osmotic current. There has been little discussion of the contribution of electro-osmosis to nanopore currents [3–5]. The electro-osmotic current of anions provides a drag which slows down the translocation of DNA through the pore. This reduces the major drawback of nanopore sequencing technology, the speed of translocation, which is often too fast to enable the detection of individual bases [3, 4]. We show here that electro-osmotic flow can dominate signals of translocation, and that under some conditions DNA in the pores of a carbon nanotube (CNT) may lead to the enhancement of the ionic current rather than to its blockade.

Single-walled carbon nanotubes (SWCNTs) are excellent candidates for nanopore applications because they have attractive chemical, electronic and mechanical properties, and can be fabricated with various lengths and diameters. Significant advantages for nanofluidic applications are based on their hydrophobic, almost frictionless internal surface. As a consequence, ionic currents through an individual

[9] Author to whom any correspondence should be addressed.

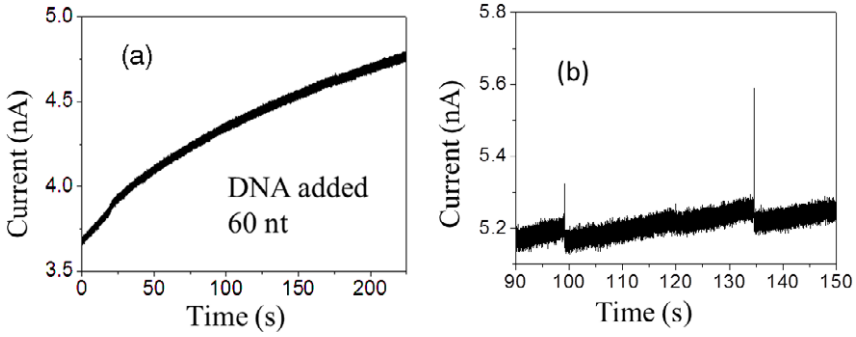

Figure 1. Measured [5] ionic current increases when ssDNA segments of ∼60 nt translocate through the metallic SWCNT of much longer length ($L = 2$ μm): (a) immediately after the addition of DNA and (b) 5 min after the addition when the current spikes appear.

SWCNT [5] are markedly different from those through other types solid-state nanopore (SSN) [6] or through protein nanopores (e.g. α-hemolysin) [7]. Firstly, the magnitude of the signal is much larger (nA) than in a conventional SSN (pA) due to a significant increase in electro-osmotic current caused by the perfect slip on the atomistically smooth internal surfaces [8], explaining, by more detailed modeling than in [5], the huge increase in the ionic current caused by surface charge at the SWCNT walls. Secondly, when DNA molecules are present in a narrow SWCNT it is observed that the ionic current may increase, opposite to the expected ionic blockade in SSN [1, 9, 10] and in protein nanopores [7]. In addition, a CNT may be much longer than the translocated DNA segments, opposite to the usual SSN applications [11]. For example, the length of the SWCNT in [5] was 2 μm, while the DNA segments were 60–120 nucleotides (nt), i.e. only ∼20–40 nm long. Therefore, the whole DNA segment typically stays inside the CNT during the translocation, which can also be related to the slow rise in ionic current (∼5 pA s^{-1}), as shown in figure 1(a) [5], later followed by the random spikes in the current flow (figure 1(b)). This can be contrasted to the usual blockade which causes a decrease of the current in the SSNs and protein nanopores.

It was speculated that the observed slow rise of the current in the experiments of Liu *et al* [5] could come from a larger number of DNA molecules that slowly build up inside the nanotube, which are then released simultaneously in 'spike' events. This raises the question of why the DNA does not swiftly translocate down the nanotube as it does in a conventional SSN. One possibility is that internal wall of the CNT gets coated by DNA. In addition, discontinuous surface charges of the CNT wall, caused by fabrication defects, could provide regions of depleted and enriched volume charge of ions, defined by the difference in concentrations of cations and anions. The dominant sign and magnitude of this volume charge is determined by competition of the CNT surface charge density and the negative charge of the DNA in the tube. This may cause focusing of the charged DNA polymer inside the CNT, and rectification of ionic current. Formation of the DNA EDL and rearrangements of electrons at the surface of the metallic CNT are also attributed to the reduction of the electrophoretic driving force at the DNA, and thus to the suppression of its translocation speed [11, 12].

The main purpose of this paper is to offer, by performing all-atoms MD simulation, a quantitative rather than a speculative study of the conditions leading to the large enhancement of ionic current during a single, short DNA translocation through a narrow, metallic SWCNT, distinct from any conventional SSN. The long-time scale of the current increase in figure 1, at the scale far beyond the nanosecond time scale of MD, is then a consequence of a cumulative buildup of many DNA segments in at successive times. This phenomenon rests on the huge variations of ionic current with electronic properties of the CNT, surface charge, radius and material of the pores which we briefly review here. A significant contribution to understanding and control of DNA translocation in the conventional SSN was given by the research of Kawai and collaborators [3, 4], aimed both at reducing the DNA translocation speed and increasing the DNA capture probability at the inlet of a SSN.

Volume exclusion of ions due to DNA and formation of a counterion layer around DNA are competing effects: the former blocks the current, while the latter increases the number of ions available for the conductance. Even in a conventional SSN, dominance of one of these effects can change the sign of the 'blockade' effect [8], depending upon the pore diameter, its material, its charge, the electrolyte concentration, and the external electric field. In addition, the effective charge density of DNA could be suppressed by almost a factor of two due to counterion screening [3, 4].

The modeled system is shown schematically in figure 2. Two reservoirs are connected by a (12, 12) single-wall CNT whose wall-center to wall-center diameter is 1.628 nm, with a length of 10 nm, resulting in 1920 carbon atoms in the tube. The system is filled with 1 M KCl solution. The ionic current is caused by the uniform electric longitudinal field E. All-atom MD simulations in the present study were performed using GROMACS 4.5.4 in an *NVT* ensemble [13]. The details of MD simulation, including a description of charging and polarization of the CNT pore surface as well as the DNA modeling, are described in the section 2. Our results are presented and discussed in section 3.

2. Computational MD method

All MD simulations in the present study were performed using GROMACS 4.5.4 in an *NVT* ensemble [13]. The

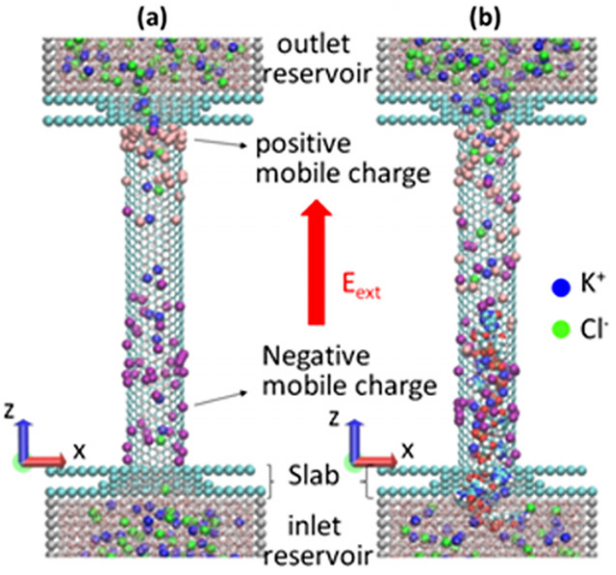

Figure 2. Schematics of the MD simulation: the SWCNT is connecting two reservoirs with solvated KCl; the system is embedded in the electrophoretic field E_{ext}; besides the fixed surface charge, the CNT also contains mobile surface charges, to allow for polarization of the CNT in the field. (a) Ionic current flows through the CNT. (b) The ionic current while DNA is translocated through the CNT.

Nośe–Hoover thermostat [14–16] was applied every 2.0 ps to maintain the system temperature at 300 K. The equations of motion were integrated using the leapfrog algorithm with a time step of 1.0 fs. The system is kept periodic only in the axial, z-direction, to preserve the number of particles N, keeping a large computation box of $20 \times 20 \times 22$ nm^3. The total number of water molecules was 11 000, which solvated 1 M KCl electrolyte (more than 200 K^+ and Cl^- ions each). The size of each reservoir is $6 \times 6 \times 6$ nm^3, and their walls are constituted of carbon atoms in a dense-packed single layer. All simulations are performed for 5.0 ns, with a sampling period of 4.0 ns (t = 1–5 ns).

For the DNA we use a 12-base single-stranded (ss) DNA of 5′-CGCGAATTCGCG-3′, which is prepared by unzipping the well-known Dickerson's B-DNA dodecamer (double stranded) [17]. The parameters (LJ parameter and atomic charge) in AMBER-99 force field [18] are used for both nonbonding pairwise interactions and boding interactions in DNA. The nonbonding interactions consist of the (6, 12) Lennard-Jones (LJ) potential and Coulombic potential. The bonding interactions are modeled with stretching, bending, and torsion. The carbon atoms in the CNT are assumed frozen and the LJ parameters are taken from Guo *et al* [19]. The slab (see figure 2) consists of united CH_2 segments and their LJ parameters are $\sigma_{\text{S–S}} = 0.3871$ nm and $\varepsilon_{\text{S–S}} = 0.4909$ kJ mol^{-1} [20]. Water molecules are modeled using the TIP3P model [21]. In the TIP3P model, the angle between hydrogen (H)–oxygen (O) vectors is fixed to 104.52°, while the distance between oxygen and hydrogen is held at 0.9572 Å. The hydrogen and oxygen charges are $+0.417e$ and $-0.834e$, respectively. The LJ parameters for K^+ and Cl^- were obtained from Koneshan *et al* [22]. The electrostatic interactions between all charged particles (including solvated ions and DNA) use a Coulomb cut-off radius of 7.5 nm.

The surface of the CNT was uniformly charged, resulting in a total surface charge Q. For example, choosing $Q = -5e$ (=–16 mC m^{-2}), the partial charge per carbon atom is $-5e/1920 = -2.6 \times 10^{-3}e$. In order to model the polarization of the metallic CNT due to the application of uniform external electric field E we placed an equal number of mobile positively and negatively charged particles of one atomic mass unit on the surface. These are allowed to move only in the axial (z) direction while constrained to the CNT surface. Motion of the particles in an azimuthal direction is also constrained to avoid head-on collisions. These particles are mutually interacting only by Coulomb, electrostatic forces. At both ends of the tube (slabs) a strong repulsive potential barrier is set to prevent escape of the mobile charged particles from the CNT surface. The 45 positive and negative particles of the same charge q_{p} are initially randomly distributed at the surface, so that $q = 45q_{\text{p}} = 0.4|Q|$. Thus, for $Q = \pm 3e$, $q = 1.20e$ and the charge of each mobile particle is $q_{\text{p}} = 1.20e/45 = 0.0267e$.

3. Results and discussion

The DNA translocation event includes the capture phase of the polymer segment by the CNT, followed by translocation through the tube ('retarded' phase [3, 4]), and the exit phase, during which the polymer leaves the tube mouth and enters the outlet reservoir. All phases of the flow may be against the strong electro-osmotic current of cations, if the CNT is negatively charged. The capture phase evolves on a much slower time scale than the retarded phase, and is also determined by probability of finding the tube mouth, by the unfolding and the entropy barrier. Capture optimization requires somewhat opposite conditions from those optimal for slowing down translocation [3, 4]. It determines the frequency of the spikes in figure 1(b), and is difficult to simulate by MD, because of the short time scale of the simulation. Therefore, in the present simulations we place the whole 11-segment DNA initially inside the tube [3], enabling its immediate translocation, which is the focus of our study rather than capture dynamics which requires a much longer time scale.

The ionic current is calculated by counting the ions that experience a complete transfer from one reservoir to another in the given time interval $\Delta t = t_2 - t_1$, where $t_1 = 1$ ns and $t_2 = 5$ ns. The total ionic current is computed by the total charge traversing the CNT, i.e. $I_{\text{tot}} = \frac{N_{\text{C}} - N_{\text{A}}}{\Delta t} e$, where $N_{\text{C,A}}$ are the signed numbers of cations and anions, respectively, which transfer ions from the inlet to outlet reservoir. $N_{\text{C,A}}$ is positive when particles move in the direction of electric field vector and negative otherwise. Particles which do not finish traveling from one reservoir to another are excluded. Those cations and anions which move opposite to and in the direction of the electric field, respectively, contribute a negative current.

As found and extensively discussed by Liu *et al* [5] and Pang *et al* [8], and also confirmed by the present MD simulations, when the tube wall is charged the ionic current is dominated by the electro-osmotic flow. The magnitude

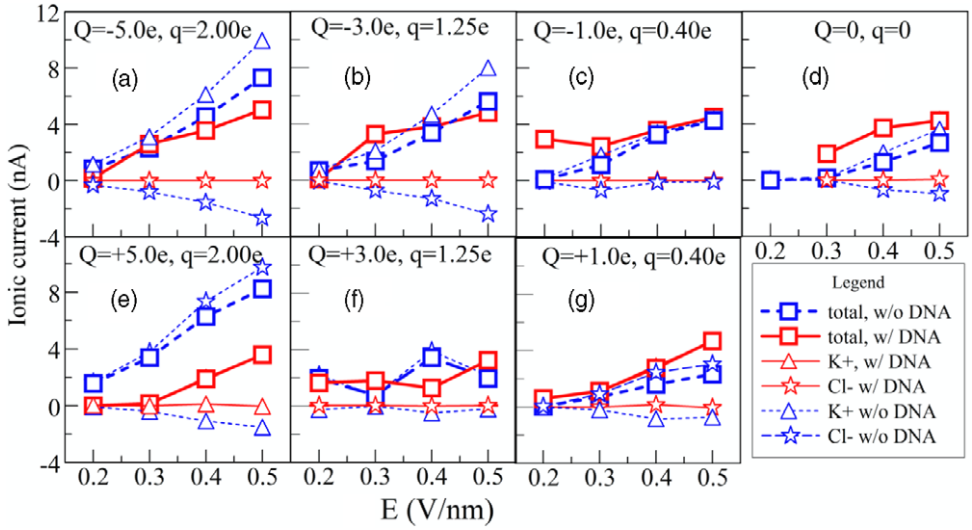

Figure 3. Ionic currents through the narrow SWCNT (dashed, blue) for various CNT surface charges Q and mobile surface charges q (see text). Ionic currents during DNA translocation are shown by solid lines (red). The symbols in the legend represent various components of the ionic current.

and sign of the charges at the walls are determined by external factors that are beyond the present simulation [8]. Therefore, we vary these charges Q in the interval from -8 to $+8 \times 10^{-19}$ C in the form of a constant charge density, supplemented by about 40% of moving charges (q) of both signs to allow for polarization of the the metallic tube in the external driving field E (details in section 2). The responses of ionic current to variation of E are shown in figure 3. Although the chosen charge densities at the surface (<16 mC m^{-2}) are small, these are compensated by the large driving fields E(0.2–0.5 V nm^{-1}), significantly higher than those reported in the Liu experiments [5]. These choices enable faster motion of ions through the tube and faster translocation, compatible with the MD (ns) time scales, providing statistically significant sampling of the ionic currents while keeping them comparable with the nA-range of measured values in figure 1. As seen in figure 3, in absence of DNA the ionic current is dominated by cations (K^+) when the CNT surface is negatively charged, and by anions (Cl^-) when the surface is positively charged.

For each set (Q, q) of surface charges and for each value of the applied electric field E we performed two sets of MD calculations, with and without a DNA segment in the tube. Comparison of the two sets of results provides insight in conditions which may cause the increases in ionic current in figure 1.

The dominant electro-osmotic flow is proportional to the driving field E and excess volume charges. The latter is induced and controlled by the EDL close to the charged tube walls (with almost perfect slip features and a Debye length of about 0.3 nm, when KCl concentration is 1 M), and also by the EDL around the DNA. Due to the no-slip features of ions around DNA, these are mainly moving together with DNA during the translocation, unlike the much faster ions close to the surface. However, since the CNT here and in the Liu *et al* experiment [5] is narrow, an overlap and mutual interactions of the two EDLs, as well as of geometrical conformations of the DNA in the CNT, can significantly influence the currents. Thus, generally, the negatively charged DNA in the tube attracts K^+, depleting Cl^- ions, and this increases the excess charge of positive ions. On the other hand, geometrical blocking, i.e. volume expulsion of the DNA, reduces the ionic current.

Coexistence and competition of the five effects explain the main features of the ionic currents in figure 3. These are (A) increase of the ionic current with E, (B) increase of ionic current with Q, where the main carrier is regulated by the sign of Q, (C) the space-charge induced by EDL of DNA, stimulating cation current, (D) volume expulsion by DNA, and (E) electrostatic repulsion of anions by DNA for positive Q.

For larger surface charges, $Q = \pm 5e$ at figures 3(a) and (e), the electro-osmotic current is large and a geometrical factor, the volume expulsion by DNA (effect D), is dominant in blocking the ionic current for both signs of Q. The blocking effect increases with electric field, i.e. with increase in ionic current due to effect (A). Both in the presence and absence of DNA, the counterions, determined by the sign of Q, are the main carriers of the current. The volume expulsion of cations is significantly smaller for negative Q, due to the space-charge effect (C above), but larger for positive Q due to electrostatic repulsion (E above).

For intermediate surface charges, $Q = \pm 3e$ (figures 3(b) and (f)), the competition of all effects (A–E above) results in both positive and negative blockades of slight magnitude, depending on the driving electric field. However, interestingly, for both signs of Q, the cation electro-osmotic current, induced by negatively charged DNA, dominates the ionic current.

However, for small charges Q at the surface, $Q = \pm 1e$, DNA causes an increased ionic current for all considered values of E, as seen in figures 3(c) and (g). As in the previous

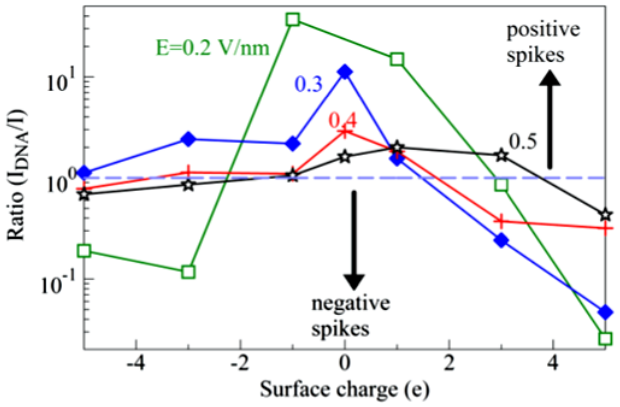

Figure 4. Ionic current enhancement factor due to the presence of a short DNA segment in the SWCNT.

case, the current in the presence of DNA is dominated by cations, irrespective of the sign of Q. In other words, cation current caused by the EDL of DNA 'normally' increases with E, playing a more significant role in inducing volume charges than the surface charge Q. In the case of positive Q, anions induced by Q are almost completely suppressed as the current carriers when DNA is present. For negative Q, the effect of enhancement is largely compensated by strong electro-osmotic current (in the absence of DNA) due to Q. Interestingly, in the absence of DNA the ionic currents are not the same for the two signs of Q. As a rule, in the case when the current is dominated by cations (negative Q) the current is somewhat larger than when it is dominated by anions. This can be attributed to a larger (by about 40%) van der Waals radius of negative Cl^- ions in comparison to the positive K^+ ions, which in the case of a narrow tube may affect both the efficiency of the DNA geometrical filtering and the electro-osmotic mobility in absence of DNA. This also explains the slight asymmetry of cation and anion currents for $Q = 0$ in figure 3(d). For that case, the cation current induced by the EDL of DNA causes a significant enhancement (negative blockade). In spite of repeated calculations, we could not get satisfactory stability of the simulations for the point at $E = 0.2$ V m^{-1} and $Q = 0$. So we decided not to show that point which does not meet the same standards of quality as the other points.

The DNA translocation effects in figure 3 are summarized in figure 4, which represents the ionic current enhancement factor due to the DNA translocation, I_{DNA}/I, as a function of the surface charge Q, for various driving fields E. A significant current increase appears for smaller surface charges Q (including the case $Q = 0$). The enhancement factors decrease with increase of E, and their peak values shift toward positive Q.

The purpose of the present work is to show that the 'ion filtering' action of just one segment 'sitting' at the exit of a narrow CNT may cause a significant ion current enhancement rather than the current blockade. This finding points out, though not conclusively, a possible mechanism for the measured increase of the current in figure 1. However, the time scale of our modeling is 4 ns, while the measurements extends to seconds, so it is difficult to draw a clear equality of the two phenomena. Future modeling, using methods adequate to much longer time scales, could show whether the measured increase in current is a consequence of the consecutive accumulation of the short-time effects obtained here. It might also show that the random current spikes [5] (shown in figure 1(b)) are evolving over a time scale many orders of magnitude longer (seconds) through the buildup of the short DNA segments (60 nt in figure 1) at the exit end of the long (2 μm) SWCNT. The cation electro-osmotic current, caused by EDL of the negatively charged DNA and possibly of the charged SWCNT surface, as well as the electrostatic barrier [8] at the tube end are opposing the exit of DNA to the reservoir (movies of supplementary information available at stacks.iop.org/Nano/23/455107/mmedia), thus indicating the accumulation of the DNA segments at the exit.

Acknowledgments

This work was supported by the DNA Sequencing Technology Program of the National Human Genome Research Institute (1RC2HG005625-01, 1R21HG004770-01), Arizona Technology Enterprises and the Biodesign Institute. This research used computational resources of the DOE National Center for Computational Sciences (NCCS) and NSF National Institute for Computational Sciences (NICS).

References

[1] Branton D *et al* 2008 The potential and challenges of nanopore sequencing *Nature Biotechnol.* **26** 1146–53
[2] Fan R, Karnik R, Yue M, Li D, Majumdar A and Yang P 2005 DNA translocation in inorganic nanotubes *Nano Lett.* **5** 1633–7
[3] He Y, Tsutsu M, Fan C, Taniguchi M and Kawai Y 2011 Controlling DNA translocation through gate modulation of nanopore wall surface charges *ACS Nano* **5** 5509–18
[4] He Y, Tsutsu M, Fan C, Taniguchi M and Kawai Y 2011 Gate manipulation of DNA capture into nanopores *ACS Nano* **5** 8391–7
[5] Liu H, He J, Tang J, Liu H, Pang P, Cao D, Krstić P S, Joseph S, Lindsay S and Nuckolls C 2010 Translocation of single-stranded DNA through single-walled carbon nanotubes *Science* **327** 64–7
[6] Dekker C 2007 Solid-state nanopores *Nature Nanotechnol.* **2** 209–15
[7] Clarke J, Wu H-C, Jayasinghe L, Patel A, Reid S and Bayley H 2009 Continuous base identification for single-molecule nanopore DNA sequencing *Nature Nanotechnol.* **4** 265–70
[8] Pang P, He J, Park J H, Krstić P S and Lindsay S 2011 Origin of giant ionic currents in carbon nanotube channels *ACS Nano* **5** 7277–83
[9] Aksimentiev A, Heng J B, Timp G and Schulten K 2004 Microscopic kinetics of DNA translocation through synthetic nanopores *Biophys. J.* **87** 2086–97
[10] Venkatesan B M and Bashir R 2011 Nanopore sensors for nucleic acid analysis *Nature Nanotechnol.* **6** 615–24
[11] Lemay S G 2010 Fluidics meets electronics: carbon nanotubes as nanopores *Angew. Chem. Int. Edn* **49** 7627–8
[12] Siwy Z S and Davenport M 2010 Making nanopores from nanotubes *Nature Nanotechnol.* **5** 174–5

[13] van der Spoel D, Lindahl E, Hess B, Groenhof G, Mark A E and Berendsen H J C 2005 GROMACS: fast, flexible, and free *J. Comput. Chem.* **26** 1701–18
[14] Hoover W G 1985 Canonical dynamics: equilibrium phase-space distributions *Phys. Rev.* A **31** 1695–7
[15] Nosé S 1984 A molecular dynamics method for simulations in the canonical ensemble *Mol. Phys.* **52** 255–68
[16] Nosé S 1984 A unified formulation of the constant temperature molecular-dynamics methods *J. Chem. Phys.* **81** 511–9
[17] Drew H R, Wing R M, Takano T, Broka C, Tanaka S, Itakura K and Dickerson R E 1981 Structure of a B-DNA dodecamer: conformation and dynamics *Proc. Natl Acad. Sci. USA* **78** 2179–83
[18] Wang J, Cieplak P and Kollman P A J 2000 How well does a restrained electrostatic potential (RESP) model perform in calculating conformational energies of organic and biological molecules *J. Comput. Chem.* **21** 1049–74
[19] Guo Y, Karasawa N and Goddard W A III 1991 Prediction of fullerene packing in C_{60} and C_{70} crystals *Nature* **351** 464–7
[20] Mashl R J, Joseph S, Aluru N R and Jakobsson E 2003 Anomalously immobilized water: a new water phase induced by confinement in nanotubes *Nano Lett.* **3** 589–92
[21] Jorgensen W L, Chandrasekhar J, Madura J D, Impley R W and Klein M L 1983 Comparison of simple potential functions for simulating liquid water *J. Chem. Phys.* **79** 926–35
[22] Koneshan S, Rasaiah J C, Lynden-Bell R M and Lee S H 1998 Solvent structure, dynamics, and ion mobility in aqueous solutions at 25 °C *J. Phys. Chem.* B **102** 4193–204